Predicting solid-state qubit material host

by

Oliver Lerstøl Hebnes

Thesis

for the degree of

Master of Science

Faculty of Mathematics and Natural Sciences
University of Oslo

March 27, 2021

Contents

Part I

Theory

Chapter 1

Quantum technologies

This chapter will provide a brief overview of the current state-of-the-art in quantum technological advances. This will not only give us insights in how the technology is being used today, but also grant us the opportunity to discuss key concepts that are fundamental to understand for this thesis. Thereafter we will look into how materials are built up, and what kind of properties a material needs to exhibit to be an eligible host for quantum devices. Finally, we will giving a few specific examples of materials with promising point defects that have been comprehensively researched. Importantly, this will motivate the reasoning for finding new materials that might excel in areas where other materials falls short for utilization in quantum technology.

Quantum technology (QT) refers to practical applications and devices that utilize the principles of quantum physics as a foundation. Technologies in this spectrum are based on concepts such as *superposition*, *entanglement* and *coherence*, which are all closely related to one another.

A quantum superposition refers to that any two or more quantum eigenstates can be added together into another valid quantum state, such that every quantum state can be represented as a sum, or a superposition, of two or more distinct states. This is according to the wave-particle duality which states that every particle or another quantum entity may be described as either a particle or a wave. When measuring the state of a system residing in a superposition of eigenstates, however, the system falls back to one of the basis states that formed the superposition, destroying the original configuration.

Quantum entanglement refers to when a two- or many-particle state cannot be expressed independently of the state of the other particles, even when the particles are separated by a significant distance. As a result, the many-particle state is termed an entangled state [1].

Quantum coherence arises if two waves coherently interfere with each other and generate a superposition of the two states with a phase relation. Likewise, loss of coherence is known as *decoherence*.

Another concept that the reader should be familiar with is the famous Heisenberg uncertainty principle. It states that

$$\sigma_x \sigma_p \geqslant \frac{\hbar}{2}, \tag{1.1}$$

where σ_x is the standard deviation for the position and σ_p is the standard deviation in momentum. This means that we cannot accurately predict both the position and momentum of a particle at the same time. Thus, we often calculate the probability for a particle to be in a state which results in concepts such as an electron sky surrounding an atom core. However, remember that equation (1.1) is an inequality, which means that it is possible to create a state where neither the position nor the momentum is well defined.

1.1 Quantum computing

The start of the digital world's computational powers can be credited to Alan Turing. In 1937, Turing [2] published a paper where he described the *Turing machine*, which is regarded as the foundation of computation and computer science. It states that only the simplest form of calculus, such as boolean Algebra (1 for true and 0 for false), is actually computable. This required developing hardware that could handle classical logic operations, and was the basis of transistors that are either in the state ON or OFF depending on the electrical signal. Equipped with a circuit consisting of wires and transistors, commonly known as a computer, we could develop software to solve all kinds of possible applications.

Driven by the development of software, conventional computers have in accordance to Moore's law [3], doubled the amount of transistors on integrated circuit chips every two years as a result of smaller transistors. Furthermore, the clock frequency has enhanced with time, resulting in a doubling of computer performance every 18 months [4]. Alas, miniaturization cannot go on forever as transistors are mass-produced at 5 nm today and are expected to reach a critical limit of 3 nm in the following years [5].

To sustain the digital world's increasing computational demand, other alternatives than the conventional classical computer must be explored. This is where quantum computing comes into the picture. The term quantum computer is a device that exploits quantum properties to solve certain computational problems more efficiently than allowed by Boolean logic [6].

The idea is to pass information in the form of a quantum bit, or *qubit* for short. They are the building blocks of quantum computers, and as opposed to the conventional 0 or 1-bits that classical computers are based on, they can inhabit any superposition of the states 0 or 1. This is illustrated in figure 1.1.

The architecture of a gate-based quantum computer is dependent on a set of quantum logic gates that perform unitary transformations on sets of qubits [7, 8]. Other implementations of quantum computers exists, such as the adiabatic quantum computer. This approach is not based on gates, but on defining the answer of a problem as the ground state of a complex network of interactions between qubits, and then controlling the interactions to adiabatically evolve the system to the ground state [9].

It has been demonstrated that exponentially complex problems can be reduced to polynomially complex problems for quantum computers [4]. For example, a quantum search algorithm found by Grover [10] offers a quadratic speed-up compared to classical algorithms, while Shor's quantum integer factorization algorithm [11] presents an exponential speed-up. Intriguingly, Google reported in 2019 that they ran a random number generator algorithm on a superconducting processor containing 53 qubits in 200 seconds, which would most likely take several times longer for a classical supercomputer to solve [12]. It is anticipated that quantum computers will excel in exceedingly complex problems, while many simpler tasks may not see any speed-up at all compared to the classical regime. Hence, quantum- and classical computers are envisioned to coexist for each their purpose.

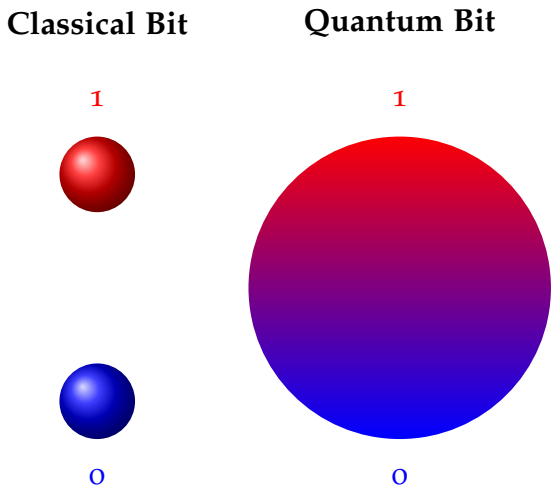

Figure 1.1: Conceptual illustration of the two-level classical bit, which are restricted to the boolean states 1 (true) or 0 (false), and the quantum bit that can be in any superposition of the states 0 or 1.

Quantum computing is a highly sought-after goal, but there are extensive challenges that needs to be adressed. Controlling a complex many-qubit system is difficult, since it is not always possible to establish interactions between qubits [7] and maintain entaglement over both time and distance. Additionally, decoherence and other quantum noise occurs as a result of the high volatility of quantum states, making quantum state manipulation prone to errors. The *quantum error correction* protocols and the theory of *threshold theorem* deals with this vulnerability, stating that noise most likely does not pose any fundamental barrier to the performance of large-scale computations [4].

1.1.1 Quantum computing requirements

As ever-promising the concepts of quantum technology are, the physical realizations are in the preliminary stage of development. Here we will concretize critical principles for a physical realisation of a quantum platform.

> "I always said that in some sense, these criteria are exactly the ones that you would teach to kindergarten children about computers, quantum or otherwise" DiVincenzo [13]

DiVincenzo formulated in the year of 2000 seven basic criteria for a physical qubit system with a logic-based architecture [7].

1. A scalable physical system with well characterized qubits
2. The ability to initialize the state of the qubits to a simple initial system
3. Have coherence times that are much longer than the gate operation time
4. Have a universal set of quantum gates
5. Have the ability to perform qubit-specific measurements

These five criteria must be met for a quantum platform to be considered a quantum computer.

1.2 Quantum communication

Quantum communication refers to the transfer of a state of one quantum system to another. Since information can be stored in qubits, we picture *flying qubits* that transfer information from one location to another [14]. The benefits of using flying qubits are in particular valued in quantum cryptography, since the quantum nature of qubits can be exploited to add extra layers of security [4].

Consider the example of encrypting a digitally transmitted conversation. It is difficult to avoid someone eavesdropping on a conversation, however, the problem is diminished if the eavesdropper does not speak the language, keeping the information in the conversation safe. This is the original idea of encryption, such that the information has been encrypted into something incomprehensible for any eavesdropper. A common practice is to encrypt information and share a public key, which everyone can read, and a private key, only known for the sender and receiver of information. This should be sufficient to keep the information secure, given that the complexity of the private key is impenetrable.

Importantly, we live in a digital world where most of our actions are increasingly being stored as information, and we could imagine that the eavesdropper in the latter example stored the conversation. Even if the content of the conversation was encrypted, it still presents a challenge, since encrypted information stored today could be deciphered in ten or twenty years' time . Consequently, finding an encryption method that could make information either impossible to eavesdrop on or make the security unbreakable forever is very desirable. This is the ultimate goal of quantum cryptography [4].

Consider the example of information encoded into a qubit as a superposition of two quantum states. Now, if a wild eavesdropper would try to measure the information, the nature of quantum physics tells us that the original configuration would be destroyed and the receiver would be alerted of the eavesdropper. Furthermore, if the eavesdropper would try to make a copy of the message, the copying itself would be limited of the no-cloning theorem [15] which declare that quantum states cannot be copied.

A clever approach to ensure confidentiality is to send the encryption key before sending the actual encrypted information. If the key is received unperturbed, the key remains secret and can be safely employed. If it turns out perturbed, confidentiality is still intact since the key does not contain any information and can be discarded. This approach is termed the *quantum key distribution* (QKD) [15, 16]. It should be noted that this requires both the sender and receiver to have access to methods for sending, receiving and storing qubit states, such as a quantum computer. Additionally, the sender and receiver will need to initially exchange a common secret which is later expanded, making quantum key *expansion* a more exact term for QKD [4, 16].

Most applications and experiments use optical fibers for sending information via photons, with the distance regarded as the main limitation. This is because classical repeaters are unable to enhance quantum information because of the no-cloning theorem, making photon loss in optical fiber cables inevitable. Thus, quantum communication must reinvent the repeater concept, using hardware that preserves the quantum nature [17] and are compatible with wavelengths used in telecommunication. Nonetheless, secure QKD up to 400 km has recently been demonstrated using optical fibres in academic prototypes [18].

1.3 Quantum sensing

Measurements are part of our digital world today to a great extent. There would be no way to exchange goods, services or information without reliable and precise measurements [17]. Thus, improving the accuracy of sensors for every measurement done is desirable. One method to improve measurement accuracy, resolution and sensitivity can be by utilizing quantum sensors.

Quantum sensors exploit quantum properties to measure a physical quantity [19]. This is possible because quantum systems are highly susceptible to pertubations to its surroundings, and can be used to detect physical properties such as either temperature or an electrical or magnetic field [19].

For a quantum system to be able to function as a quantum sensors, a few criterias needs to be met. Firstly, the quantum system needs to have discrete and resolvable energy levels. The quantum system also needs to be controllably initialised into a state that can be identified and coherently manipulated by time-dependent fields. Lastly, the quantum system needs to be able to interact with the physical property one wants to measure through a coupling parameter [19].

It is also possible to also exploit quantum entanglement to improve the precision of a measurement. This gain of precision is used to reach what is called the Heisenberg-limit, which states that the precision scales as the number of particles N in an idealized quantum system [17, 19], while the best classical sensors scale with $\sqrt{N}$.

1.4 Available quantum platforms

Many different quantum platforms have been physically implemented, and this section will serve as a brief overview of the current status. For a more thorough review of qubit implementations, the reader is directed to Refs. [8, 17].

Superconducting circuits can be used in quantum computing, since electrons in superconducting materials can form Cooper pairs via an effective electron-electron attraction when the temperature is lower than a critical limit. Below the limit, electrons can move without resistance in the material [20]. Exploiting this intrinsic coherence, qubits can be made by forming microwave circuits based on loops of two superconducting elements separated by an insulator, also known as Josephson tunnel junctions [17]. Today, superconducting Josephson junctions are the most widely used quantum platform, but they requires very low temperature (mK) to function, making them costly to use. Additionally, the current devices experience a relatively short coherence time, causing challenges in scaling up.

Single photons is an eligible quantum platform that can be implemented as qubits with one-qubit gates being formed by rotations of the photon polarization. Its use in fiber optics are less prone to decoherence, but faces challenges since the more complex photon-photon entanglement and control of multi-qubits is strenuous [8].

By fixing the nuclear spin of solid-state systems, it is possible to implement a quantum platform that experience long spin coherence. This enables the manipulation of qubits that utilize electromagnetic fields, making one-qubit gates realizable.

The isolated atom platform is characterized by its well-defined atom isolation. Here, every qubit is based on energy levels of a trapped ion or atom. Quantum entanglement can be achieved through laser-induced spin coupling, however scaling up to large atom numbers induce problems in controlling large systems and cooling of the trapped atoms or ions.

A quantum dot (QD) can be imagined as an artifical atom which is confined in a solid-state host. As an example, a quantum dot can occur when a hole or an electron is trapped in the localized potential of a semiconductor's nanostructure. QDs exhibit similar coherence potential as the isolated atom platform, but without the drawback of confining and cooling of the given atom or ion [17]. Moreover, it is possible to limit decoherence due to nuclear spins by dynamic decoupling of nuclear spin noise and isotope purification [8].

A QD can normally be defined litographically using metallic gates, or as self-assembled QDs where a growth process creates the potential that traps electrons or holes. The difference between them is a question of controllability and temperature, since the metallic gates is primarily controlled electrically and operate at < 1 K, while self-assembly QDs are primarily controlled optically at ~ 4 K [8]. Despite requiring very low temperatures, QDs have the potential for fast voltage control and opticial initialization. As with trapped ions, electrostatically defined quantum dots experience a short-range exchange interaction, imposing a limitation for quantum computing and quantum error correction protocols. A potential solution could include photonic connections between quantum dots. On the contrary, self-assembled quantum dots couple strongly to photons due to their large size in comparison to single atoms. However, the size and shapes of self-assembled quantum dots are decided randomly during the growth process, causing an unfavourable large range of optical absorption and emission energies [8].

Lastly, we will turn towards point defects in bulk semiconductors as a physical implementation of a quantum platform. Point defects shares many of the attributes of quantum dots, such as discrete optical transitions and controllable coherent spin states, but are vulnerable to small changes in the lattice of the semiconductor. Thus, it can be difficult to isolate a point defect from the surrounding environment. However, one can utilize the strength of the solid-

state semiconductor host to isolate to some extent the point defect, yielding extended coherence times and greater optical homogeneity than other quantum dot systems. Before we dwell into the intricacies of point defect qubits as a building block for QT, we will provide the neccessary background for the crystal- and electronic structure of semiconductors.

1.5 Introduction to semiconductor physics

The interactions between atoms and characteristics of matter form the foundation of materials science. The applications of materials science are extensive, with examples such as a bottle of water or to a chair to sit in.

Solid materials, like plastic bottles, are formed by densely packed atoms. These atoms can randomly occur through the material without any long-range order, which would categorize the material as an *amorphous solid*. Amorphous solids are frequently used in gels, glass and polymers [21]. However, the atoms can also be periodically ordered in small regions of the material, classifying the material as a *polycrystalline solid*. All ceramics are polycrystalline with a broad specter of applications ranging from kitchen-porcelain to orthopedical bio-implants [22]. A third option is to have these atoms arranged with infinite periodicity, making the material a *crystalline solid* or more commonly named a *crystal*. The three options are visualised in figure 1.2. Hereon, we will focus on crystalline solids.

The periodicity in a crystal is defined in terms of a symmetric array of points in space called the *lattice*, which can be simplified as either a one-dimensional array, a two-dimensional matrix or a three dimensional vector space, depending on the material. At each lattice point we can add an atom to make an arrangement called a *basis*. The basis can be one atom or a cluster of atoms having the same spatial arrangement. Every crystal has periodically repeated building blocks called *cells* representing the entire crystal. The smallest cell possible is called a *primitive cell*, but such a cell only allows lattice points at its corners and it is often quite rigid to work with when the structure becomes complex. As a solution, we will consider the *unit cell*, which allows lattice points on face centers and body centers.

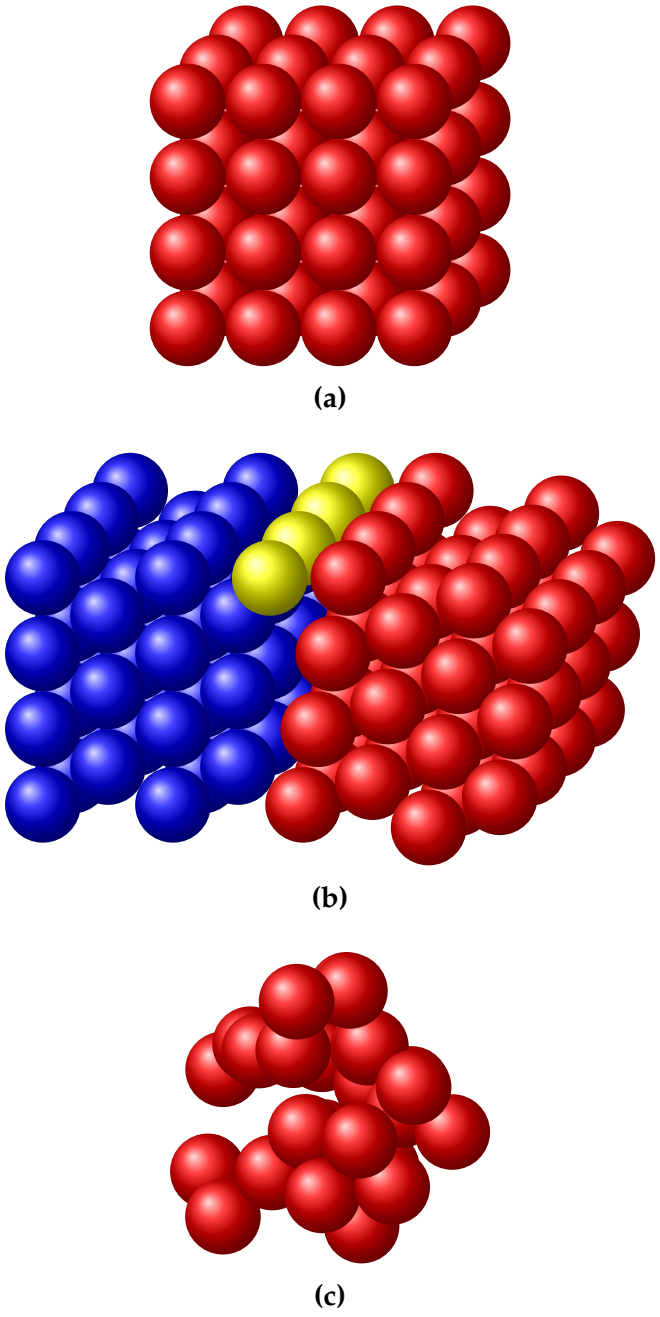

Figure 1.2: Schematic representation of different degrees of ordered structures, where (a) is a crystalline of a simple cubic lattice, (b) is a polycrystalline hexagonal lattice, and (c) is an amorphous lattice.

One example of a crystal structure is the perovskite structure. Compounds with this structure are characterized by having an ABX_3 stoichiometry whose symmetri belong to one of 15 space groups identified by Lufaso & Woodward [23], such as the cubic, orthorombic and tetragonal. For our purpose, we will be looking into when the X atom is oxygen, and refer to the oxygen-perovskite ABO_3. The A atom is nine- to 12-fold coordinated by oxygen, while the B atom is sixfold coordinated by oxygen, and the BO_6 octahedra are connected to the corners in all three directions as visualized in figure 1.3.

The motivation behind the research on perovskites is related to the large amount of available ABO_3 chemistries, where a significant portion of these take the perovskite structure. Perovskites have a broad specter of applications, ranging from high-temperature superconductors [24] and ionic conductors [25] to multiferroic materials [26]. Additionally, adding a perovskite-type compound to solar cells has reportedly resulted in higher performance efficiencies while being cheap to produce and simple to manufacture [27, 28]. However, this includes the use of hybrid organic-inorganic compounds and excludes the use of oxygen.

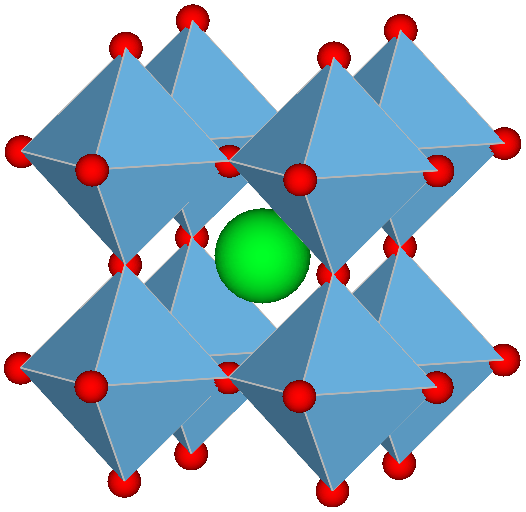

Figure 1.3: A crystal structure of $SrTiO_3$ which is a cubic perovskite. The red atoms are oxygen, whereas the green atom is strontium, and inside every corner-sharing BO_6 octahedral unit is a titanium atom.

Isolated atoms have distinct energy levels, where the Pauli exlusion principle [29] states for fermions that each energy level can at most accomodate two electrons of opposite spin. In a solid, the discrete energy levels of the isolated atom spread into continuous energy bands since the wavefunctions of the electrons in the neighboring atoms overlap. Hence, an electron is not neccessarily localized at a particular atom anymore. This is examplified as every material has a unique band structure, similar to every human having their unique fingerprint.

Knowing which energy bands are occupied by electrons is the key in understanding the electrical properties of solids. The highest occupied electron band at 0 K is called the valence band (VB), while the lowest unoccupied electron band is called the conduction band (CB). The energy gap of forbidden energy levels between the maximum VB and the minimum CB is known as the band gap, and its energy is denoted as E_g. If a material can be classified

as a semiconductor depends on the band gap and the electrical conductivity. As an example, Silicon is commonly thought of as a semiconductor, and has a band gap of about 1.12 eV at 275 K [30].

To be able to accelerate electrons in a solid using an electrical field, they must be able to move into new energy states. At 0 K, the entire valence band of a semiconductor is full with electrons and there are no available states nearby, making it impossible for current to flow through the material. This can be solved by using either thermal or optical energy to excite electrons from the valence band to the conduction band, in order to *conduct* electricity. At room temperature, some semiconductors will have electrons excited to the conduction band solely from thermal energy matching the energy band gap [21].

In some scenarios, thermal or optical energy is not sufficient for an excitation since the energy bands are also dependent on the crystal momentum. A difference in the momentum of the minimal-energy state in the conduction band and the maximum-energy state in the valence band results in an *indirect bandgap* as seen in figure 1.4a. If there is no difference at all, the material has a *direct bandgap*, which is visualized in figure 1.4b.

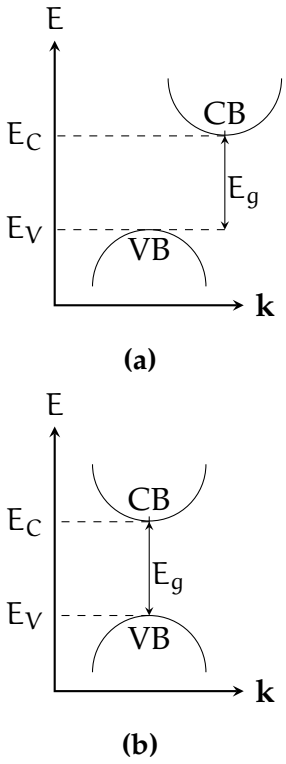

Figure 1.4: A schematic drawing of (a) an indirect- and (b) a direct bandgap.

Electrons in semiconductor materials can be described according to the Fermi-Dirac distribution

$$f(E) = \frac{1}{1 + e^{(E-E_F)/kT}},$$

where k is Boltzmann's constant, T is temperature, E is the energy and E_F is the Fermi level. The Fermi-Dirac distribution gives the probability that a state will be occupied by an electron, and at $T = 0$ K, every energy state lower than E_F is occupied by electrons while the opposite is true for energy states above E_F [21].

1.5.1 Point defects in semiconductors

In real life, a perfect crystal without any symmetry-breaking flaw does not exist. These flaws are known as defects and can occur up to three dimen-

sions. An example one-dimensional defect is known as a *line defect*, while two dimensional defects can be *planar defects*, and in three dimensions we have *volume defects*. Lastly, defects can also occur in zero dimensions and are then termed *point defects*. Point defects normally occur as either vacancies, interstitial placement inbetween lattice sites or as substitution of another existing atom in the lattice.

Defects can greatly influence both the electronic and optical propertires of a material. A substitional defect can at first be regarded as an impurity or an antisite, but they can also be intentionally inserted, an approach known as *doping*. Doping can result in an excess of electrons or holes, making the semiconductor either an n- or p-type, respectively. Consequently, the semiconductor will have energy levels in the (forbidden) band gap that originates from the defects. If the energy levels introduced are closer than ~ 0.2 eV to the band egdes, they are termed *shallow* defects.

Shallow defects can contribute with either excess electrons to the conduction band, or excess holes to the valence band. However, the induced charge carriers (electrons or holes) interact strongly with the band egdes, resulting in a delocalized wavefunction regarding the position in the lattice.

For the opposite case, if the energy levels rests closer to the middle of the semiconductor's gap, the introduced defects are known as *deep level* defects. Deep levels normally occur due to either dangling bonds or impurities, and have highly localized electron wavefunctions. This might assure the isolation required for long coherence times, which is an appealing promise in quantum technological advances.

Deep levels can be unfortunate in semiconductors since they can interact with the charge carriers, potentially destroying the desired electronic or optical property of the material. Deep level defects can function as electron-hole recombination centers, or to trap charge carriers, yielding the commonly used name deep level *traps*. Both of the given situations results in a lower concentration of charge carriers, which showcase why deep levels can be unwanted in semiconductor devices. However, deep level defects show extraordinary properties in Q

1.5.2 Optical defect transitions

Optical transitions refers to excitation of charge carriers due to either emission or absorption of electromagnetic radiation, and can be done with a laser light or electron beam. Figure 1.5 represents a configuration coordinate (CC) diagram of a defect transition. The y-axis is a function of the energy E, while the x-axis is a function of the configuration coordination Q. The lowest point in the lower parabola is known as the ground state (GS) configuration Q_{GS}, which is the most stable atomic position, while for the upper parabola it

is known as the excited state configuration Q_{ES}. The dotted lines represent vibronic excitations to the energy of the ground state Q_{GS} for the lower parabola, while it represents Q_{ES} for the higher parabola.

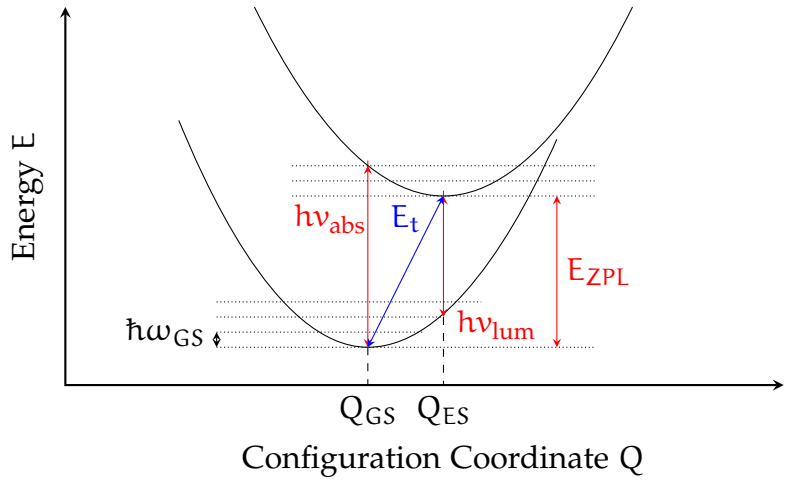

Figure 1.5: A schematic representation of a configuration coordination diagram based on Ref. [31].

The optical transitions in figure 1.5 are marked with red arrows. During slow transitions, such as during thermodynamic defect transitions, the original configuration have time to rearrange due to phonon vibrations. This is schematically drawn as the blue arrow, where the energy E_t equals the ionization energy or the position of the defect level. Optical transitions, on the other hand, are marked in red and occur in a short time range such that the original configuration does not change. They can appear in the exchange of charge carriers with the band egdes, and in a defect's internal excited state, with the latter scenario being most relevant for this thesis.

Consider a defect that rests in the ground state configuration Q_{GS}. Suddenly, it absorbs a photon with energy $h\nu_{abs}$ and occupies an excited vibronic state of the upper parabola after a vertical transition. Through lattice reconfigurations, the defect will move towards the bottom of the upper parabola, also known as Q_{ES}. Eventually, it will relax to the lower parabola by emitting a photon with energy $h\nu_{lum}$, also known as a zero-phonon line (ZPL) of energy E_{ZPL}. On the other hand, any transitions between vibronic excitation levels are phonon-related. How strong the electron-phonon interaction is can be quantified by the Huang-Rhys factor S [32]. If the two parabolas in figure 1.5 have the same configuration of Q, emission into the ZPL is enabled and $S \sim 0$. The stronger the coupling, the smaller amount of emission in the ZPL.

The optical properties of a host material can be greatly influenced by defects, in particular the ES to GS transition that can occur in a defect, as discussed for figure 1.5. If the defect were to fascilitate the emission of single

photons with a detectable time inbetween together with a distinguishable ZPL, the defect would be referred to as a single photon source (SPS). The criteria for SPS are not met in many materials, since charge-state transitions often comprise interactions with either the VB or the CB. Thus, most SPSs' GS and ES levels are situated within the band gap of a host material. Consequently, mostly wide-band gap semiconductors are used as host materials for SPSs.

1.6 Semiconductor candidates for quantum technology

The properties of point defects are promising in a quantum technological perspective. We have seen that point defects fasciliate deep energy levels within the band gap of the semiconductor, and provide isolation in the solid-state matrix as a result from a high degree of localization of the defect orbitals. If the host material have a small spin-orbit coupling, it could provide long coherence times for a deep level trap in localized and high-spin states. Additionally, point defects have the potential to be single-photon sources, giving rise to sharp and distinguishable optical transitions, where a significant amount of the emission can be of the energy E_{ZPL}. This is in particular seen in wide-bandgap semiconductors, and combined with a weak electron-phonon interaction, can have the capacity to be fabricated as a high-fidelity SPS with a significant ZPL part.

The most studied point defect system is the nitrogen-vacancy (NV^{-1}) in diamond. Figure 1.6 schematically shows the different stages of constructing the negative charge state. Panel 1.6a shows the electronic states that correspond to the difference for an isolated atom and a lattice of atoms, as a superposition of sp^3 orbitals that generates valence and conduction bands. In panel 1.6b, a vacancy has been created by removing a carbon atom, and the four orbitals interact with each other resulting in two new states with a_1 and t_2 symmetry due to dangling bonds. Substituting a carbon atom with a nitrogen atom further splits the t_2-states into two new states. The states $a(1)$ and $e_{x'}e_y$ are of importance, as they are the GS and the ES of the qubit defects, respectively. Here, an optical spin-conserving transition can occur due to a laser light of correct wavelength [33], as exemplified from the discussion from the last section.

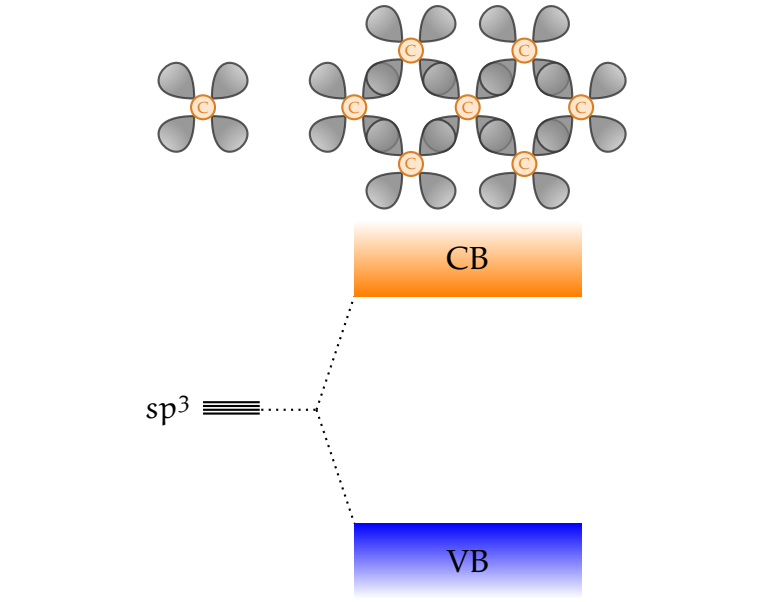

(a)

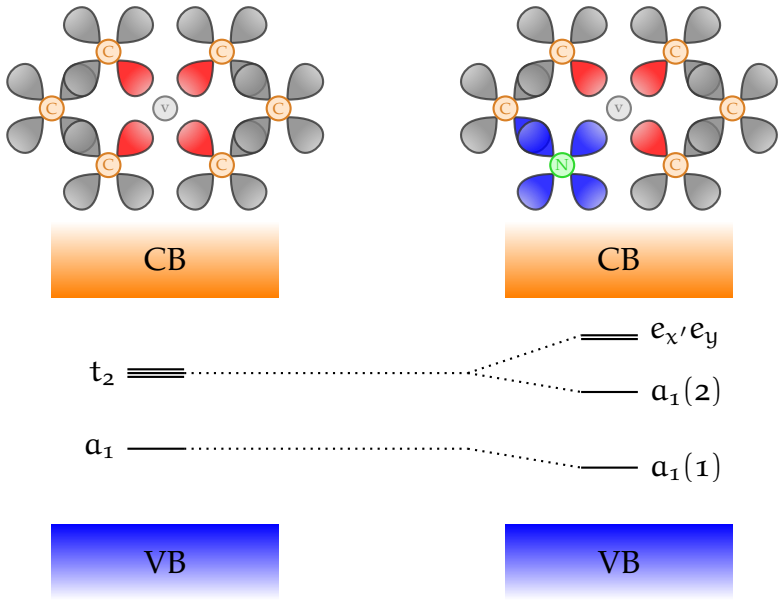

(b)

Figure 1.6: A schematic representation of the electronic structure of the NV^{-1} defect in a tetrahedrally coordinated semiconductor, exemplified by diamond. Figure used from Ref. [33].

The nitrogen-vacancy in diamond is a prominent single-photon source up to room temperatures. This involves initializing, manipulating and reading out of the qubit state using optical and electric excitations, and electric and magnetic fields [33]. The potential qubit system have promising applications in quantum- communication and computation, with a demonstrated entanglement between two NV center spins that are separated by 3 m [34]. Nevertheless, perhaps the most propitious application can be seen in quantum sensing as high-sensivity magnetometer with nanoscale resolution [35].

Unfortunately, the NV-center display restricted capababilities for quantum communication and computation. The amount of emission into the zero-phonon line is 4% at 6 K [36], which is low. The emission of the qubit center is not completely compatible with current optical fiber technologies, since the emission is in the red wave-length specter. Additionally, fabricating materials of diamond is far from unchallenging and serves as a signficant incentive to find other promising qubit candidates.

1.6.1 Qubit material host requirements

Therefore, we turn to the search of other QT compatible hosts that offers similar capabilities, but that are more user-friendly. In particular, we need to search for new promising materials that can host a potential point defect. Weber *et al.* [6] proposed in 2010 four criteria that should be met for a solid-state semiconductor material hosting a qubit defect, whereas some of the criteria has already been discussed. An ideal crystalline host should have [6]

(H1) A wide-band gap to accomodate a deep center.

(H2) Small spin-orbit coupling in order to avoid unwanted spin flips in the defect bound states.

(H3) Availability as high-quality, bulk, or thin-film single crystals.

(H4) Constituent elements with naturally occuring isotopes of zero nuclear spin.

Table (1.1) lists several material host candidates that exhibit promising band gap capable of accommodating a deep level defect. The spin-orbit splitting is an indication of the strength of the spin-orbit interaction, and is taken at the Γ point from the valence-band splitting. A smaller value may indicate less susceptibility to decoherence.

Criterion (H3) is important for scalability and further potential for a large-scale fabrication. The given candidate hosts provided in table (1.1) can all be grown as single crystals, but with varying quality and size.

Material	Band gap E_g (eV)	Spin-orbit splitting Δ_{so} (meV)	Stable spinless nuclear isotopes?
3C-SiC	2.39	10	Yes
4H-SiC	3.26 [37]	6.8	Yes
6H-SiC	3.02	7.1	Yes
AlN	6.13	19 [38]	No
GaN	3.44	17.0	No
AlP	2.45	50 [39]	No
GaP	2.27	80	No
AlAs	2.15	275	No
ZnO	3.44 [40]	-3.5	Yes
ZnS	3.72 [41]	64	Yes
ZnSe	2.82	420	Yes
ZnTe	2.25	970	Yes
CdS	2.48	67	Yes
C (Diamond)	5.5	6	Yes
Si	1.12	44	Yes

Table 1.1: Table taken from Gordon *et al.* [33] that lists a number of tetrahedrally coordinated hosts whose band gaps are larger than 2.0 (eV), and compares it to diamond and Si. All experimental values are from Ref. [30], except for where explicity cited otherwise.

Normally, nuclear spin is a major source of decoherence for all semiconductor-based quantum technologies. This would exclude the use of all elements in odd groups in the periodic table, since these elements exhibit nonzero nuclear spin. As a result, the spin-coherence time of a paramagnetic deep center [6] might increase. However, nuclear spin can also induce additional quantum degrees of freedom for applications in the right configuration [42]. Therefore, criterion (H4) is not a strict requirement but is a general recommendation for reducing decoherence time.

Weber *et al* [6] use criteria $(H1) - (H4)$ to specifically find analogies to the NV^{-1} center in other material systems, thus leaving the discussion of other criteria out, such as the choice of crystal system. The atomic configuration and crystal structure of a material strongly influences the properties of a defect, since a defect's orbital and spin structure is dependent on its spatial symmetry [42]. In particular, it is the point group that decides which multiplicity a given energy level should have [43]. A higher defect symmetry group generally facilitates degenerate states, which may give rise to high spin states according to Hund's rules [42, 44]. Inversion symmetry in the host crystal can also be beneficial, resulting in reduced inhomogenous broadening and

spectral diffusion of optical transitions as a consequence of being generally insensitive to external electric fields [42].

1.6.2 Silicon carbide

Silicone carbide (SiC) is an emerging quantum platform that exists in a wide variety of polytypes, with 3C, 4H and 6H being the most prominent configurations. Several of the polytypes have been demonstrated to host SPEs with a slightly different emitter characteristic, which provides the opportunity to select the desired properties based on the variety of lattice configurations and point defects available [6, 45, 46]. While 3C has a cubic structure, we find 4H in a hexagonal structure with both hexagonal (h) and pseudo-cubic (k) lattice sites. 6H is found in a hexagonal structure with the three orientations that are labelled h, k_1 and k_2. Importantly, SiC in the three varieties experience wide-band gaps, low spin orbit coupling and stable spinless nuclear isotopes [6, 30, 37], as seen from table 1.1. Furthermore, SiC benefits from mature fabrication on the wafer-scale, which checks the last of the four (H1-H4) QT host requirements, marking it as a suitable quantum material platform.

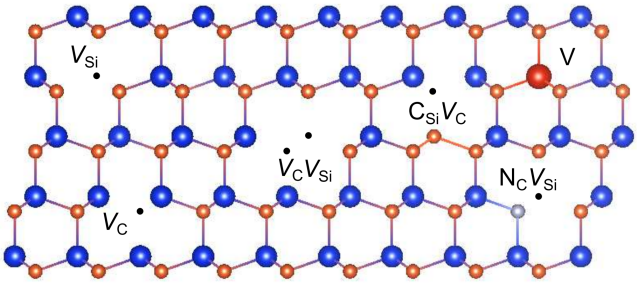

Figure 1.7: Schematic illustration of various point defects in 4H-SiC, where Si atoms are blue while C atoms are orange. The illustration includes the point defects Si vacancy (V_{Si}), C vacancy (V_C), divacancy ($V_{Si}V_C$), carbon antisite-vacancy pair ($C_{Si}V_C$), nitrogen-vacancy (N_CV_{Si}) and the vanadium impurity (V).

The most studied emitters in SiC include the carbon antisite-vacancy pair $C_{Si}V_C$ that emits in the red, the silicon vacancy V_{Si} that emits in the near infra-red, and the divacancy ($V_{Si}V_C$) and the nitrogen-vacancy center (N_CV_{Si}) that both emit at near-telecom wavelengths. Thus, the two latter emitters could potentially ease the integration with optic fiber technologies as compared to e.g. the NV^-. Additionally, the four different point defects have all been identified as room-temperature SPEs with demonstrated coherent spin control [47]. Illustrations of several configurations of emitters in 4H-SiC are included in figure 1.7.

1.6.3 Other materials

Single photon emitters have been observed in other semiconductor materials, however most of the emitters are yet to be identified or are in an early stage of identification. Therefore, specific details about spin- or emission-related structure are yet to be implemented. In this section we will briefly mention recent promising materials for QT.

One immediate potential candidate is silicon, considering the favorable device fabrication processes that are available. It has demonstrated that phosphorous impurities at Si sites can store a quantum state for over 30 seconds, enabling their use in a potential Kane quantum computer [48]. Unfortunately, the P impurity lack any single photon source capabilities. Recently, however, the G-center arising from the carbon-interstitial carbon-substitutional (C_sC_i) complex was identified as an promising SPE candidate with single photon emissions at telecom wavelength [49].

Other materials that emits individual photons have been detected in other wide-band gap semiconductors, including ZnO, ZnS, GaN and AlN [48]. Unfortunately, challenges due to the specific materials complicate the implementation of defects for QT. ZnO and ZnS experience a broad emission due to a large photon involvement. GaN and AlN, on the other hand, are more susceptible to a more narrow emission, where room-temperature SPE has been demonstrated for both GaN [50] and wurtzite AlN films [51]. The defect levels for AlN films have been tentatively assigned to the nitrogen-vacancy and divacancy complexes, but they tend to occur too close to the band edges for any SPE [48, 52].

Two-dimensional materials such as hexagonal boron nitride (h-BN) are also of interest as quantum platforms [53]. The structure exists in single- or multilayers, and it has been demonstrated a broad range of stable room-temperature single-photon emitters [54, 55]. However, secure identification for the source of the emission is yet to be established [56, 57].

1.6.4 Associated challenges with material host discovery

The idea of finding new potential host candidates to utilise point defects in QT is of a challenging sort. Recall, we have made four criteria that deals with the required (H1) band gaps, (H2) spin-orbit coupling, (H3) availability and (H4) spin-zero isotopes, but we have no knowledge of if there should be more criteria or to what extent a criteron needs to be fulfilled. What we do know is that there are major advantages if materials exhibit properties such as isolation in the lattice and weak electron-photon interaciton, however, the process to provide any quantity of measurements are through approximations and material-specific properties. These approximations does not neccessarily capture quantum properties well.

Furthermore, the identified candidates constitues an immensely selective group with only a handful potential hosts. As an example, all known potential hosts are unary or binary. This is probably due to the increasing complexity dealing with an additional level of interactions in the lattice. It is not to avoid that quantum technology is in its preliminary phase of development. Therefore, there are reasons to believe that many potential hosts are yet to be discovered.

Part II

Appendices

Appendix A

Featurizaton

A.1 Table of featurizers

Table A.1: This thesis' chosen 39 featurizers from matminer. Descriptions are either found from Ref. [58] or from the project's Github page.

Features	Description	Original reference
Composition features		
AtomicOrbitals	Highest occupied molecular orbital (HOMO) and lowest unoccupied molecular orbital (LUMO).	[59]
AtomicPacking-Efficiency	Packing efficiency.	[60]
BandCenter	Estimation of absolute position of band center using geometric mean of electronegativity.	[61]
ElementFraction	Fraction of each element in a composition.	-
ElementProperty	Statistics of various element properties.	[62–64]
IonProperty	Maximum and average ionic character.	[63]

Continued on next page

Table A.1 – continued from previous page

Features	Description	Original reference
Miedema	Formation enthalpies of intermetallic compounds, solid solutions, and amorphous phases using semi-empirical Miedema model.	[65]
Stoichiometry	L^p norm-based stoichiometric attributes.	[63]
TMetalFraction	Fraction of magnetic transition metals.	[64]
ValenceOrbital	Valence orbital attributes such as the mean number of electrons in each shell.	[63]
YangSolid-Solution	Mixing thermochemistry and size mismatch terms.	[66]
Oxid composition features		
Electronegativity-Diff	Statistics on electronegativity difference between anions and cations.	[64]
OxidationStates	Statistics of oxidation states.	[64]
Structure features		
DensityFeatures	Calculate density, volume per atom and packing fraction.	-
GlobalSymmetry-Features	Determines spacegroup number, crystal system (1-7) and inversion symmetry.	-
RadialDistribution-Function	Calculates the radial distribution function of a crystal system.	-
CoulombMatrix	Generate the Coulomb matrix, which is a representation of the nuclear coulombic interaction of the input structure.	[67]
PartialRadial-Distribution-Function	Compute the partial radial distribution function of a crystal structure	[68]

Continued on next page

Table A.1 – continued from previous page

Features	Description	Original reference
SineCoulomb-Matrix	Computes a variant of the coulomb matrix developed for periodic crystals.	[69]
EwaldEnergy	Computes the energy from Coulombic interactions based on charge states of each site.	[70]
BondFractions	Compute the fraction of each bond in a structure, based on nearest neighbours.	[71]
Structural-Heterogeneity	Calculates the variance in bond lengths and atomic volumes in a structure.	[72]
MaximumPacking-Efficiency	Calculates the maximum packing efficiency of a structure.	[72]
ChemicalOrdering	Computes how much the ordering of species differs from random in a structure.	[72]
XRDPowder-Pattern	1D array representing normalized powder diffraction of a structure as calculated by pymatgen.	[62]
Site features		
AGNI-Fingerprints	Calculates the product integral of RDF and Gaussian window function	[73]
AverageBond-Angle	Determines the average bond angle of a specific site with its nearest neighbors using pymatgens implementation.	[74]
AverageBond-Length	Determines the average bond length between one specific site and all its nearest neighbors using pymatgens implementation.	[74]
BondOrientational-Paramater	Calculates the averages of spherical harmonics of local neighbors	[75, 76]

Continued on next page

Table A.1 – continued from previous page

Features	Description	Original reference
ChemEnvSite Fingerprint	Calculates the resemblance of given sites to ideal environment using pymatgens ChemEnv package.	[77, 78]
Coordination-Number	The number of first nearest neighbors of a site	[78]
CrystalNN-Fingerprint	A local order parameter fingerprint for periodic crystals.	-
GaussianSymm-Func	Calculates the gaussian radial and angular symmetry functions originally suggested for fitting machine learning potentials.	[79, 80]
GeneralizedRadial-Distribution-Function	Computes the general radial distribution function for a site	[75]
LocalProperty-Difference	Computes the difference in elemental properties between a site and its neighboring sites.	[72, 74]
OPSite-Fingerprint	Computes the local structure order parameters from a site's neighbor environment.	[78]
Voronoi-Fingerprint	Calculates the Voronoi tessellation-based features around a target site.	[81, 82]
Density of state features		
DOSFeaturizer	Computes top contributors to the density of states at the valence and conduction band edges. Thus includes chemical specie, orbital character, and orbital location information.	[83]
Band structure features		

Continued on next page

Table A.1 – continued from previous page

Features	Description	Original reference
BandFeaturizer	Converts a complex electronic band structure into quantities such as band gap and the norm of k point coordinates at which the conduction band minimum and valence band maximum occur.	-

A.2 Erroneous entries

MPID	Full formula	Reference
mp-555563	$PH_6C_2S_2NCl_2O_4$	[84]
mp-583476	$Nb_7S_2I_{19}$	[85]
mp-600205	$H_{10}C_5SeS_2N_3Cl$	-
mp-600217	$H_{80}C_{40}Se_8S_{16}Br_8N_{24}$	-
mp-1195290	$Ga_3Si_5P_{10}H_{36}C_{12}N_4Cl_{11}$	-
mp-1196358	$P_4H_{120}Pt_8C_{40}I_8N_4Cl_8$	-
mp-1196439	$Sn_8P_4H_{128}C_{44}N_{12}Cl_8O_4$	-
mp-1198652	$Te_4H_{72}C_{36}S_{24}N_{12}Cl_4$	-
mp-1198926	$Re_8H_{96}C_{24}S_{24}N_{48}Cl_{48}$	-
mp-1199490	$Mn_4H_{64}C_{16}S_{16}N_{32}Cl_8$	-
mp-1199686	$Mo_4P_{16}H_{152}C_{52}N_{16}Cl_{16}$	-
mp-1203403	$C_{121}S_2Cl_{20}$	-
mp-1204279	$Si_{16}Te_8H_{176}Pd_8C_{64}Cl_{16}$	-
mp-1204629	$P_{16}H_{216}C_{80}N_{32}Cl_8$	-

Table A.2: A table of manually identified entries from Materials Project that experience issues concerning Matminer's featurization tools. These were excluded from the dataset.

Bibliography

1. Griffiths, D. *Introduction to quantum mechanics* ISBN: 9781107179868 (Cambridge University Press, Cambridge, 2017).
2. Turing, A. M. On computable numbers, with an application to the Entscheidungsproblem. *Proceedings of the London mathematical society* **2,** 230–265 (1937).
3. Moore, G. Cramming More Components Onto Integrated Circuits. *Proceedings of the IEEE* **86,** 82–85 (Jan. 1965).
4. Pavičić, M. *Quantum computation and quantum communication : theory and experiments* ISBN: 9786610743704 (Springer, New York, 2006).
5. Gwennap, L. Apple's 5 Nanometer Chip Is Another Signpost That Moore's Law Is Running Out. *Forbes.* <https://www.forbes.com/sites/linleygwennap/2020/10/12/apple-moores-law-is-running-out/> (Oct. 12, 2020).
6. Weber, J. R. *et al.* Quantum computing with defects. *Proceedings of the National Academy of Sciences* **107,** 8513–8518 (Apr. 2010).
7. DiVincenzo, D. P. The Physical Implementation of Quantum Computation. *Fortschritte der Physik* **48,** 771–783 (Sept. 2000).
8. Ladd, T. D. *et al.* Quantum computers. *Nature* **464,** 45–53 (Mar. 2010).
9. Mizel, A., Lidar, D. A. & Mitchell, M. Simple Proof of Equivalence between Adiabatic Quantum Computation and the Circuit Model. *Physical Review Letters* **99.** doi:10.1103/physrevlett.99.070502 (Aug. 2007).
10. Grover, L. K. A framework for fast quantum mechanical algorithms. arXiv: quant-ph/9711043v2 [quant-ph] (Nov. 20, 1997).
11. Shor, P. *Algorithms for quantum computation: discrete logarithms and factoring* in *Proceedings 35th Annual Symposium on Foundations of Computer Science* (IEEE Comput. Soc. Press, 1994). doi:10.1109/sfcs.1994.365700.
12. Martinis, J. M. *et al. Quantum supremacy using a programmable superconducting processor* en. 2019. doi:10.5061/DRYAD.K6T1RJ8.
13. Georgescu, I. The DiVincenzo criteria 20 years on. *Nature Reviews Physics* **2,** 666–666 (Nov. 2020).

14. Griffiths, R. B. Nature and location of quantum information. *Physical Review A* **66.** doi:10.1103/physreva.66.012311 (July 2002).

15. Gisin, N., Ribordy, G., Tittel, W. & Zbinden, H. Quantum cryptography. *Reviews of Modern Physics* **74,** 145–195 (Mar. 2002).

16. Gisin, N. & Thew, R. Quantum communication. *Nature Photonics* **1,** 165–171 (Mar. 2007).

17. Acín, A. *et al.* The quantum technologies roadmap: a European community view. *New Journal of Physics* **20,** 080201 (Aug. 2018).

18. Boaron, A. *et al.* Secure Quantum Key Distribution over 421 km of Optical Fiber. *Physical Review Letters* **121.** doi:10.1103/physrevlett.121.190502 (Nov. 2018).

19. Degen, C. L., Reinhard, F. & Cappellaro, P. Quantum sensing. *Reviews of Modern Physics* **89.** doi:10.1103/revmodphys.89.035002 (July 2017).

20. Kristian Fossheim, A. S. *Superconductivity: Physics and Applications* 442 pp. ISBN: 0470844523. <https://www.ebook.de/de/product/3608091/kristian_fossheim_asle_sudboe_superconductivity_physics_and_applications.html> (WILEY, 2004).

21. Ben Streetman, S. B. *Solid State Electronic Devices, Global Edition* 632 pp. ISBN: 1292060557. <https://www.ebook.de/de/product/30394493/ben_streetman_sanjay_banerjee_solid_state_electronic_devices_global_edition.html> (Pearson Education Limited, 2015).

22. Renganathan, G., Tanneru, N. & Madurai, S. L. in *Fundamental Biomaterials: Metals* 211–241 (Elsevier, 2018). doi:10.1016/b978-0-08-102205-4.00010-6.

23. Lufaso, M. W. & Woodward, P. M. Prediction of the crystal structures of perovskites using the software program SPuDS. *Acta Crystallographica Section B Structural Science* **57,** 725–738 (Nov. 2001).

24. Bednorz, J. G. & Müller, K. A. Perovskite-type oxides—The new approach to high-Tcsuperconductivity. *Reviews of Modern Physics* **60,** 585–600 (July 1988).

25. Boivin, J. C. & Mairesse, G. Recent Material Developments in Fast Oxide Ion Conductors. *Chemistry of Materials* **10,** 2870–2888 (Oct. 1998).

26. Cheong, S.-W. & Mostovoy, M. Multiferroics: a magnetic twist for ferroelectricity. *Nature Materials* **6,** 13–20 (Jan. 2007).

27. Ibn-Mohammed, T. *et al.* Perovskite solar cells: An integrated hybrid lifecycle assessment and review in comparison with other photovoltaic technologies. *Renewable and Sustainable Energy Reviews* **80,** 1321–1344 (Dec. 2017).

28. Chen, P.-Y. *et al.* Environmentally responsible fabrication of efficient perovskite solar cells from recycled car batteries. *Energy Environ. Sci.* **7,** 3659–3665 (2014).

29. Pauli, W. Über den Zusammenhang des Abschlusses der Elektronengruppen im Atom mit der Komplexstruktur der Spektren. *Zeitschrift für Physik* **31,** 765–783 (Feb. 1925).

30. Martienssen, W. *Springer handbook of condensed matter and materials data* ISBN: 9786610625949 (Springer, Heidelberg New York, 2005).

31. Pelant, I. *Luminescence spectroscopy of semiconductors* ISBN: 0191738549 (Oxford University Press, Oxford, 2012).

32. Kun Huang, A. R. Theory of light absorption and non-radiative transitions in F -centres. *Proceedings of the Royal Society of London. Series A. Mathematical and Physical Sciences* **204,** 406–423 (Dec. 1950).

33. Gordon, L. *et al.* Quantum computing with defects. *MRS Bulletin* **38,** 802–807 (Oct. 2013).

34. Bernien, H. *et al.* Heralded entanglement between solid-state qubits separated by three metres. *Nature* **497,** 86–90 (Apr. 2013).

35. Taylor, J. M. *et al.* High-sensitivity diamond magnetometer with nanoscale resolution. *Nature Physics* **4,** 810–816 (Sept. 2008).

36. Barclay, P. E., Fu, K.-M. C., Santori, C., Faraon, A. & Beausoleil, R. G. Hybrid Nanocavity Resonant Enhancement of Color Center Emission in Diamond. *Physical Review X* **1.** doi:10.1103/physrevx.1.011007 (Sept. 2011).

37. Neudeck, P. G. Progress in silicon carbide semiconductor electronics technology. *Journal of Electronic Materials* **24,** 283–288 (Apr. 1995).

38. Silveira, E., Freitas, J. A., Glembocki, O. J., Slack, G. A. & Schowalter, L. J. Excitonic structure of bulk AlN from optical reflectivity and cathodoluminescence measurements. *Physical Review B* **71.** doi:10.1103/physrevb.71.041201 (Jan. 2005).

39. Lawaetz, P. Valence-Band Parameters in Cubic Semiconductors. *Physical Review B* **4,** 3460–3467 (Nov. 1971).

40. Beckers, L. *et al.* Structural and optical characterization of epitaxial waveguiding BaTiO3 thin films on MgO. *Journal of Applied Physics* **83,** 3305–3310 (Mar. 1998).

41. Kumbhojkar, N., Nikesh, V. V., Kshirsagar, A. & Mahamuni, S. Photophysical properties of ZnS nanoclusters. *Journal of Applied Physics* **88,** 6260–6264 (Dec. 2000).

42. Bassett, L. C., Alkauskas, A., Exarhos, A. L. & Fu, K.-M. C. Quantum defects by design. *Nanophotonics* **8,** 1867–1888 (Oct. 2019).

43. James, W. J. Theory of defects in solidsby A. M. Stoneham. *Acta Crystallographica Section A* **32,** 527–527 (May 1976).

44. Togan, E. *et al.* Quantum entanglement between an optical photon and a solid-state spin qubit. *Nature* **466,** 730–734 (Aug. 2010).

45. Son, N. T. *et al.* Developing silicon carbide for quantum spintronics. *Applied Physics Letters* **116,** 190501 (May 2020).

46. Falk, A. L. *et al.* Polytype control of spin qubits in silicon carbide. *Nature Communications* **4.** doi:10.1038/ncomms2854 (May 2013).

47. Widmann, M. *et al.* Coherent control of single spins in silicon carbide at room temperature. *Nature Materials* **14,** 164–168 (Dec. 2014).

48. Zhang, G., Cheng, Y., Chou, J.-P. & Gali, A. Material platforms for defect qubits and single-photon emitters. *Applied Physics Reviews* **7,** 031308 (Sept. 2020).

49. Redjem, W. *et al.* Single artificial atoms in silicon emitting at telecom wavelengths. *Nature Electronics* **3,** 738–743 (Nov. 2020).

50. Berhane, A. M. *et al.* Photophysics of GaN single-photon emitters in the visible spectral range. *Physical Review B* **97.** doi:10.1103/physrevb.97.165202 (Apr. 2018).

51. Xue, Y. *et al.* Single-Photon Emission from Point Defects in Aluminum Nitride Films. *The Journal of Physical Chemistry Letters* **11,** 2689–2694 (Mar. 2020).

52. Varley, J. B., Janotti, A. & de Walle, C. G. V. Defects in AlN as candidates for solid-state qubits. *Physical Review B* **93.** doi:10.1103/physrevb.93.161201 (Apr. 2016).

53. Toth, M. & Aharonovich, I. Single Photon Sources in Atomically Thin Materials. *Annual Review of Physical Chemistry* **70,** 123–142 (June 2019).

54. Tran, T. T. *et al.* Robust Multicolor Single Photon Emission from Point Defects in Hexagonal Boron Nitride. *ACS Nano* **10,** 7331–7338 (July 2016).

55. Tran, T. T., Bray, K., Ford, M. J., Toth, M. & Aharonovich, I. *Quantum Emission from Hexagonal Boron Nitride Monolayers* in *Conference on Lasers and Electro-Optics* (OSA, 2016). doi:10.1364/cleo_qels.2016.ftu4d.1.

56. Weston, L., Wickramaratne, D., Mackoit, M., Alkauskas, A. & de Walle, C. G. V. Native point defects and impurities in hexagonal boron nitride. *Physical Review B* **97.** doi:10.1103/physrevb.97.214104 (June 2018).

57. Abdi, M., Chou, J.-P., Gali, A. & Plenio, M. B. Color Centers in Hexagonal Boron Nitride Monolayers: A Group Theory and Ab Initio Analysis. *ACS Photonics* **5,** 1967–1976 (Apr. 2018).

58. Ward, L. *et al.* Matminer: An open source toolkit for materials data mining. *Computational Materials Science* **152,** 60–69 (Sept. 2018).

59. Kotochigova, S., Levine, Z. H., Shirley, E. L., Stiles, M. D. & Clark, C. W. Local-density-functional calculations of the energy of atoms. *Physical Review A* **55,** 191–199 (Jan. 1997).

60. Laws, K. J., Miracle, D. B. & Ferry, M. A predictive structural model for bulk metallic glasses. *Nature Communications* **6.** doi:10.1038/ncomms9123 (Sept. 2015).

61. Butler, M. A. & Ginley, D. S. Prediction of Flatband Potentials at Semiconductor-Electrolyte Interfaces from Atomic Electronegativities. *Journal of The Electrochemical Society* **125,** 228–232 (Feb. 1978).

62. Ong, S. P. *et al.* Python Materials Genomics (pymatgen): A robust, open-source python library for materials analysis. *Computational Materials Science* **68,** 314–319 (Feb. 2013).

63. Ward, L., Agrawal, A., Choudhary, A. & Wolverton, C. A general-purpose machine learning framework for predicting properties of inorganic materials. *npj Computational Materials* **2.** doi:10.1038/npjcompumats.2016.28 (Aug. 2016).

64. Deml, A. M., O'Hayre, R., Wolverton, C. & Stevanović, V. Predicting density functional theory total energies and enthalpies of formation of metal-nonmetal compounds by linear regression. *Physical Review B* **93.** doi:10.1103/physrevb.93.085142 (Feb. 2016).

65. Weeber, A. W. Application of the Miedema model to formation enthalpies and crystallisation temperatures of amorphous alloys. *Journal of Physics F: Metal Physics* **17,** 809–813 (Apr. 1987).

66. Yang, X. & Zhang, Y. Prediction of high-entropy stabilized solid-solution in multi-component alloys. *Materials Chemistry and Physics* **132,** 233–238 (Feb. 2012).

67. Rupp, M., Tkatchenko, A., Müller, K.-R. & von Lilienfeld, O. A. Fast and Accurate Modeling of Molecular Atomization Energies with Machine Learning. *Physical Review Letters* **108.** doi:10.1103/physrevlett.108.058301 (Jan. 2012).

68. Schütt, K. T. *et al.* How to represent crystal structures for machine learning: Towards fast prediction of electronic properties. *Physical Review B* **89.** doi:10.1103/physrevb.89.205118 (May 2014).

69. Faber, F., Lindmaa, A., von Lilienfeld, O. A. & Armiento, R. Crystal structure representations for machine learning models of formation energies. *International Journal of Quantum Chemistry* **115,** 1094–1101 (Apr. 2015).

70. Ewald, P. P. Die Berechnung optischer und elektrostatischer Gitterpotentiale. *Annalen der Physik* **369,** 253–287 (1921).

71. Hansen, K. *et al.* Machine Learning Predictions of Molecular Properties: Accurate Many-Body Potentials and Nonlocality in Chemical Space. *The Journal of Physical Chemistry Letters* **6,** 2326–2331 (June 2015).

72. Ward, L. *et al.* Including crystal structure attributes in machine learning models of formation energies via Voronoi tessellations. *Physical Review B* **96.** doi:10.1103/physrevb.96.024104 (July 2017).

73. Botu, V. & Ramprasad, R. Adaptive machine learning framework to accelerate ab initio molecular dynamics. *International Journal of Quantum Chemistry* **115,** 1074–1083 (Dec. 2014).

74. De Jong, M. *et al.* A Statistical Learning Framework for Materials Science: Application to Elastic Moduli of k-nary Inorganic Polycrystalline Compounds. *Scientific Reports* **6.** doi:10.1038/srep34256 (Oct. 2016).

75. Seko, A., Hayashi, H., Nakayama, K., Takahashi, A. & Tanaka, I. Representation of compounds for machine-learning prediction of physical properties. *Physical Review B* **95.** doi:10.1103/physrevb.95.144110 (Apr. 2017).

76. Steinhardt, P. J., Nelson, D. R. & Ronchetti, M. Bond-orientational order in liquids and glasses. *Physical Review B* **28,** 784–805 (July 1983).

77. Waroquiers, D. *et al.* Statistical Analysis of Coordination Environments in Oxides. *Chemistry of Materials* **29,** 8346–8360 (Sept. 2017).

78. Zimmermann, N. E. R., Horton, M. K., Jain, A. & Haranczyk, M. Assessing Local Structure Motifs Using Order Parameters for Motif Recognition, Interstitial Identification, and Diffusion Path Characterization. *Frontiers in Materials* **4.** doi:10.3389/fmats.2017.00034 (Nov. 2017).

79. Behler, J. Atom-centered symmetry functions for constructing high-dimensional neural network potentials. *The Journal of Chemical Physics* **134,** 074106 (Feb. 2011).

80. Khorshidi, A. & Peterson, A. A. Amp: A modular approach to machine learning in atomistic simulations. *Computer Physics Communications* **207,** 310–324 (Oct. 2016).

81. Peng, H. L., Li, M. Z. & Wang, W. H. Structural Signature of Plastic Deformation in Metallic Glasses. *Physical Review Letters* **106.** doi:10.1103/physrevlett.106.135503 (Mar. 2011).

82. Wang, Q. & Jain, A. A transferable machine-learning framework linking interstice distribution and plastic heterogeneity in metallic glasses. *Nature Communications* **10.** doi:10.1038/s41467-019-13511-9 (Dec. 2019).

83. Dylla, M. T., Dunn, A., Anand, S., Jain, A. & Snyder, G. J. Machine Learning Chemical Guidelines for Engineering Electronic Structures in Half-Heusler Thermoelectric Materials. *Research* **2020,** 1–8 (Apr. 2020).

84. None Available. *Materials Data on PH6C2S2N(ClO2)2 by Materials Project* en. 2020. doi:10.17188/1268877.

85. None Available. *Materials Data on Nb7S2I19 by Materials Project* en. 2014. doi:10.17188/1277059.